JOURNAL OF GUIDANCE, CONTROL, AND DYNAMICS
Vol. 21, No. 1, January–February 1998

Use of Energy-State Analysis on a Generic Air-Breathing Hypersonic Vehicle

David K. Schmidt* and Jochen A. Hermann†
University of Maryland, College Park, Maryland 20742

A possible next-generation launch vehicle may be a fully reusable, single-stage-to-orbit aerospacecraft. This class of hypersonic vehicle includes highly integrated airframe and propulsion systems; hence fuel-optimal trajectories are of special interest. Also, because these vehicles are neither conventional aircraft nor rockets, the appropriate approach for trajectory analysis during preliminary design, for example, is of interest. Addressed here is whether the energy-state method is justified for the determination of such trajectories for scramjet-powered, hypersonic vehicles. The focus is on the scramjet-powered phase of the mission. The energy-state approach is known to be justified when the system dynamics exhibit multi-time-scale behavior, and such behavior is shown to exist for the vehicle and mission phase under investigation here. Furthermore, solutions obtained via the energy-state assumption are compared with a full dynamic solution obtained using a nonlinear programming routine. It is shown that the results from the two methods are in reasonably good agreement. On the basis of these results, the energy-state method would appear justified for the class of vehicle in question, at least for obtaining rapid performance estimates, as well as gaining insight into the basic performance issues.

Nomenclature

C_{T_x}	= vehicle x-thrust coefficient
C_{T_z}	= vehicle z-thrust coefficient
D	= aerodynamic drag
E	= vehicle energy height
g	= gravitational acceleration
h	= altitude
I_{sp}	= specific impulse
L	= aerodynamic lift
m	= vehicle mass
R	= distance from Earth's center
Th	= engine thrust
t	= time
t_i	= characteristic time constant of state i
V	= velocity
W	= vehicle weight
$\dot{W}_f$	= fuel flow rate
w_i	= characteristic weight constant of state i
$X_{\text{plume}}, Z_{\text{plume}}$	= forces due to exhaust plume pressure distribution
$X_{\text{turn}}, Z_{\text{turn}}$	= forces due to turning of flow at engine inlet
α	= vehicle angle of attack
γ	= vehicle flight-path angle
ε	= singular perturbation parameter
μ	= gravitational constant for Earth

Introduction

A POSSIBLE next-generation launch vehicle may be a fully reusable, single-stage-to-orbit (SSTO) aerospacecraft. One of the major design issues for this class of vehicle will be maximizing the payload to orbit. Hence fuel-optimal trajectories are of special interest. The highly integrated airframe and propulsion systems that are typical of these vehicles lead to highly interacting airframe and engine characteristics. And the feasibility of such a mission relies heavily on the efficient operation, e.g., trajectory shaping, of such a vehicle.[1,2]

Received Sept. 29, 1995; revision received July 10, 1997; accepted for publication July 25, 1997.

*Professor of Aerospace Engineering and Director, Flight Dynamics and Control Laboratory. Associate Fellow AIAA.

†Visiting Graduate Research Assistant, Flight Dynamics and Control Laboratory. Student Member AIAA.

Because these vehicles are neither conventional aircraft nor rockets, the appropriate approach for trajectory analysis during preliminary design, for example, is of particular interest. The specific problem to be addressed in this paper is whether the energy-state method is justified as an appropriate method for estimating such optimal trajectories for a generic, hypersonic lifting-body configuration, powered with scramjet propulsion. If so, this approach has the advantage of offering considerable insight into the critical design features affecting the vehicle performance.

The energy-state approach is closely related to the singular perturbation technique[3] and is justified when the system dynamics have widely separated time scales. This characteristic of the system in question will be investigated, and the focus will be on the scramjet-powered phase of the mission. Furthermore, solutions obtained via the energy-state assumption will be compared with a full dynamic solution obtained using a nonlinear programming routine.[4] It will be shown that these results compare quite favorably. Hence, the use of the energy-state approximation for this vehicle and mission phase appears justified, in contrast to the conclusions of Ref. 5.

Vehicle and Mission Characteristics

The SSTO mission involves delivering payload into low Earth orbit with a single-stage vehicle. To maximize the orbital mass fraction (or payload to orbit), minimum-fuel trajectories are of special interest. The side view of the generic, scramjet-powered hypersonic vehicle to be considered here is shown in Fig. 1. The vehicle geometry (cf. Ref. 6) was selected to reflect key characteristics similar to those of the X-30 vehicle. The configuration is a lifting body, consisting of a forebody/engine inlet, internal scramjet engine module, and afterbody/exhaust nozzle. The gross weight of the vehicle at scramjet ignition is taken to be 300,000 lb, and the length of the vehicle is 150 ft.

The vehicle's lower forebody surface both produces aerodynamic lift and acts as a precompression surface upstream of the inlet to the engine. The afterbody/nozzle surface experiences exhaust-plume impingement, which produces both propulsive thrust and "lift." These two design characteristics lead to strong interactions between the propulsion system and the airframe. Specifically, with reference to Fig. 1, total propulsive thrust and lift are

$$T_x = \text{Th} + X_{\text{plume}} + X_{\text{turn}}, \qquad T_z = Z_{\text{plume}} + Z_{\text{turn}} \tag{1}$$

Therefore, the total force normal to the velocity vector is

$$L_{\text{avail}} = L + (\text{Th} + X_{\text{turn}} + X_{\text{plume}})\sin(\alpha) - (Z_{\text{plume}} + Z_{\text{turn}})\cos(\alpha) \tag{2}$$

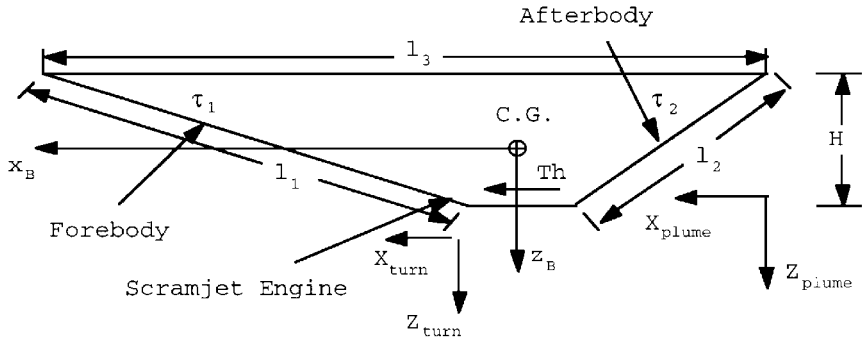

Fig. 1 Hypersonic vehicle configuration.

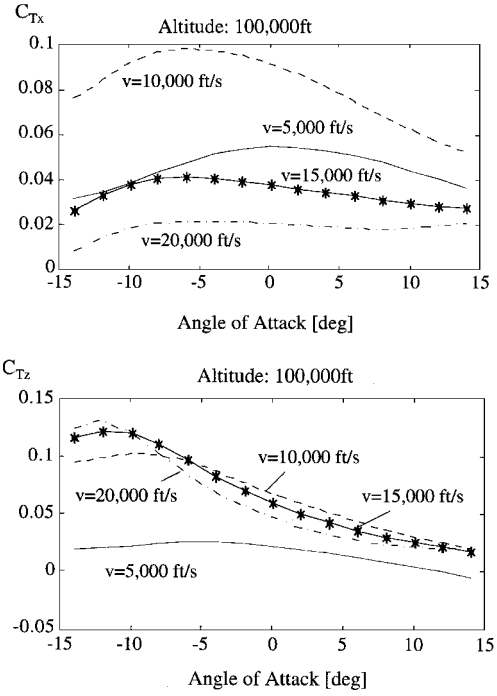

Fig. 2 Propulsive force coefficients.

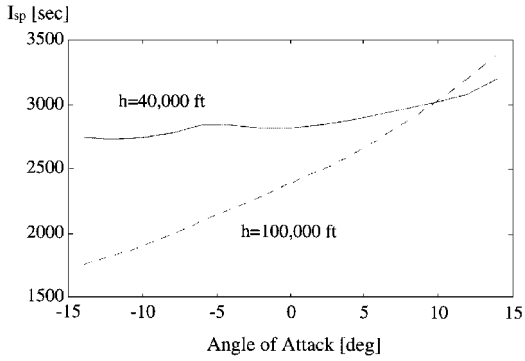

Fig. 3 Specific impulse (V = 10,000 ft/s).

If coefficients C_{T_x} and C_{T_z} are the propulsive forces nondimensionalized by flight dynamic pressure and the aerodynamic reference area, Fig. 2 shows typical values of these coefficients, corresponding to 100,000-ft altitude. Coefficients corresponding to lower altitudes take on smaller values. The specific impulse is

$$I_{\text{sp}} = \frac{1}{\dot{W}_f}[(\text{Th} + X_{\text{plume}} + X_{\text{turn}})\cos\alpha + (Z_{\text{plume}} + Z_{\text{turn}})\sin\alpha] \equiv \frac{\text{Th}_{\text{installed}}}{\dot{W}_f} \tag{3}$$

Note that this relationship includes the component of thrust along the velocity vector. Figure 3 shows the specific impulse corresponding to a flight velocity of 10,000 ft/s at two different altitudes. The angle-of-attack dependence is greater at higher altitudes, where the reduced atmospheric density magnifies the effect of the precompression from the forebody. The main points to be noted with respect to the data are that these propulsive forces are strong functions of vehicle angle of attack, and the propulsive lift is the same order of magnitude as, but in the opposite direction from, the aerodynamic lift.

Energy-State Approximation

The energy-state method (cf. Ref. 7) is a simple graphical approach for rapidly estimating the solution to a trajectory-optimization problem. Both minimum-time and minimum-fuel trajectories can be obtained. One key advantage is that the method enhances physical insight into the factors dominating the vehicle's performance. But hypersonic air-breathing vehicles are quite different from conventional aircraft, to which this method has typically been applied. Of special note are the differences in thrust-to-weight ratios and in the flight velocities for the two classes of vehicles. Therefore, before applying the energy-state method to this new kind of aerospacecraft, it must be shown that the necessary assumptions are valid.

Under a point-mass assumption, and considering only motion in a vertical plane, the equations governing the vehicle motion over a spherical nonrotating Earth are[8]

$$\dot{E} = \frac{(\text{Th}_{\text{installed}} - D)V}{W} \tag{4}$$

$$\dot{h} = V\sin\gamma \tag{5}$$

$$\dot{\gamma} = (g/WV)[L_{\text{avail}} - W\cos\gamma] + [V/R]\cos\gamma \tag{6}$$

$$\dot{W} = -\dot{W}_f \tag{7}$$

where we take the energy height to be

$$E = h + (V^2/2g) \tag{8}$$

In the time domain, the validity of the energy-state approximation hinges on the existence of multi-time-scale behavior. Specifically, it is assumed that flight-path angle γ and altitude h are arbitrarily fast, and the weight is arbitrarily slow, all compared with energy height E. Under these assumptions, the fourth-order system can be reduced to a single equation, Eq. (4). Typically, vertical force equilibrium is assumed, which for a given weight W_0 leads to

$$L + (\text{Th} + X_{\text{plume}} + X_{\text{turn}})\sin\alpha - (Z_{\text{plume}} + Z_{\text{turn}})\cos\alpha = W_0 - (mV^2/R) \tag{9}$$

The time required to transition from energy height E_0 to E_f is

$$\Delta t = \int_{E_0}^{E_f} \mathrm{d}t \qquad \text{where} \qquad \mathrm{d}t = \frac{\mathrm{d}E}{\dot{E}} \tag{10}$$

Table 1 Summary of parameters for characteristic time calculations

State	$x_{\min}$	$x_{\max}$	$\dot{x}_i$	Comments
E	5.0×10^5 ft	10.0×10^6 ft	$\dot{E} = (V/W_0)\,\mathrm{Th}_{\mathrm{avail}}$	$W_0 = 150{,}000$ lb
h	20,000 ft	200,000 ft	$\dot{h} = V$	Set $\sin\gamma = 1$
γ	-1.57 rad	1.57 rad	$\dot{\gamma} = (g/VW_0)\,\mathrm{L}_{\mathrm{effective}}$	Set $\cos\gamma = 1$ $W_0 = 150{,}000$ lb
W	50,000 lb	300,000 lb	$\dot{W} = -\dot{W}_f$	——

Therefore, to minimize flight time for a given energy change, $\dot{E}$ should be maximized at each energy height. The fuel required to transition from E_0 to E_f is

$$W_f = \int_{E_0}^{E_f} \mathrm{d}W_f = \int_{E_0}^{E_f} \frac{\mathrm{d}E}{\mathrm{d}E/\mathrm{d}W_f} \tag{11}$$

where the ratio $\mathrm{d}E/\mathrm{d}W_f$ is the energy gained per unit weight of fuel burned, at a given energy height E. Thus the fuel required to increase the total energy is minimized by maximizing $(\mathrm{d}E/\mathrm{d}W_f)$ $(=\dot{E}/\dot{W}_f)$ at each energy level along the trajectory, and hence this problem is solved in the weight domain. The system in this case is just Eqs. (4–6), all divided by Eq. (7). This system can be reduced to order 1 (the energy-state approximation) if the change in flight path and altitude can occur with little weight change compared with an energy change, or $\mathrm{d}E/\mathrm{d}W_f$ is small compared with $\mathrm{d}h/\mathrm{d}W_f$ and $\mathrm{d}\gamma/\mathrm{d}W_f$.

Multi-Time/Weight-Scale Behavior

By examining Eqs. (4–7), the critical parameters noted are thrust-to-weight ratio T/W, lift-to-weight ratio L/W, flight velocity V, and fuel flow rate (determined by specific fuel consumption). For conventional aircraft, T/W is of order 1 or less, whereas L/W can be greater than 1. Hence, it is not surprising that the necessary time-scale behavior is exhibited for such vehicles. However, for a hypersonic vehicle the velocity can be 15–25 times that of a conventional aircraft. Furthermore, $\dot{E}$ is proportional to V, whereas $\dot{\gamma}$ is inversely proportional to V. Hence, it is not a priori clear by inspection whether the multi-time-scale behavior exists. And, in fact, in Ref. 5 the authors concluded that this behavior could only be guaranteed to exist if the maximum axial acceleration of the vehicle was less than unity (1 g). For the vehicle in question, the maximum axial acceleration is about 5. Hence, more careful analysis is required.

Furthermore, we wish to assess the presence of the requisite behavior prior to solving for the optimal trajectory. That is, we wish to determine if the energy-state assumptions are valid in general, not just along some prescribed trajectory. For the vehicle in question, the state rates $\dot{E}$, $\dot{h}$, $\dot{\gamma}$, and $\dot{W}$ have been determined over the feasible range of angle of attack. These rates are shown in Fig. 4 for one example flight condition, $h = 60{,}000$ ft and $V = 10{,}000$ ft/s. The altitude rate $\dot{h} = V\sin\gamma$ is always of order V, or 10,000 ft/s. Clearly, some states are significantly faster than others in the units chosen.

But more care is required in determining "fast" and "slow." The range over which each state transitions must also be considered. The approach suggested here is to find a characteristic time constant for each state. Such time constants are the inverse of state velocities, used, for example, in Ref. 9 and elsewhere. By defining the range over which each state varies, each rate can be converted into the time required to span that range. These ranges are, of course, mission dependent. For the generic hypersonic vehicle described previously and the mission of interest, the suggested ranges are given in Table 1.

Now given the state velocities from the equations of motion [Eqs. (4–7)], evaluated at a given flight condition, a characteristic time constant

$$t_i = \Delta x_i/\dot{x}_i \tag{12}$$

for each state can be calculated. If these characteristic time constants differ significantly, and if this difference is observed over the entire flight envelope, the existence of multi-time-scale behavior would be supported.

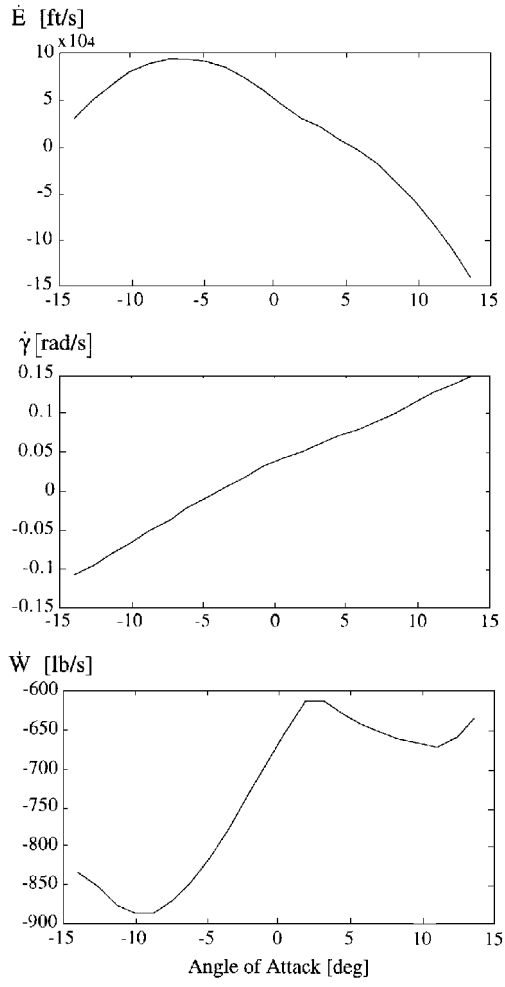

Fig. 4 State rates at h = 60,000 ft and V = 10,000 ft/s.

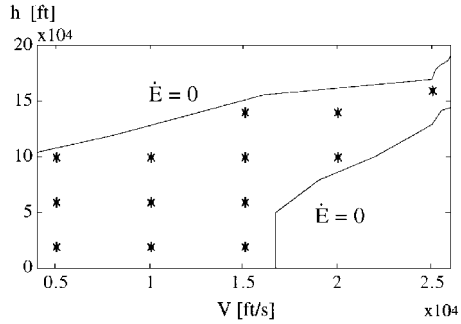

Fig. 5 Flight envelope.

Figure 5 shows the selected points in the flight envelope to be considered, and Table 2 gives the main results. At each flight condition, an angle of attack always exists such that h and γ are significantly faster (hence have smaller time constants) than E and W. Furthermore, the difference in the characteristic times t_h and t_γ compared with t_E and t_W is typically one order of magnitude at all points. Table 2 also reveals that at all points in the flight envelope, except at point 7, weight changes more slowly than energy.

Table 2 Characteristic times at different points in the flight envelope

Point	h, ft	V, ft/s	t_E, s	t_h, s	t_γ, s	t_W, s	α, rad
1	20,000	5,000	532	36	55	1,260	−0.105
			975	36	9	1,021	0.001
2	60,000	5,000	737	36	66	2,666	−0.012
			799	36	58	2,702	0.004
3	100,000	5,000	3,302	36	244	13,682	−0.060
			3,624	36	401	14,768	0.009
4	20,000	10,000	89	18	27	137	−0.126
			54	18	5	81	0.012
5	60,000	10,000	337	18	30	412	0.036
			230	18	35	393	0.018
6	100,000	10,000	173	18	64	527	−0.150
			725	18	150	1,254	0.160
7	20,000	15,000	76	12	38	49	−0.065
			2,340	12	11	59	−0.112
8	60,000	15,000	179	12	40	225	−0.110
9	100,000	15,000	141	12	61	410	−0.108
			679	12	252	830	0.077
10	140,000	15,000	548	12	77	693	−0.244
			326	12	194	1,167	0.001
11	100,000	20,000	169	9	42	320	−0.135
			5,388	9	525	702	0.026
12	140,000	20,000	391	9	60	479	−0.198
			307	9	218	1,139	0.001
13	160,000	25,000	426	7	86	630	−0.153
			380	7	277	1,514	0.001

Table 3 Minimum characteristic times at different points in the flight envelope

Point	h, ft	V, ft/s	t_E, s	t_h, s	t_γ, s	t_W, s
1	20,000	5,000	526	36	7	948
2	60,000	5,000	622	36	30	2,612
3	100,000	5,000	3,293	36	112	13,681
4	20,000	10,000	45	18	3	72
5	60,000	10,000	100	18	15	282
6	100,000	10,000	168	18	47	527
7	20,000	15,000	76	12	7	44
8	60,000	15,000	177	12	14	186
9	100,000	15,000	141	12	32	339
10	140,000	15,000	268	12	77	653
11	100,000	20,000	164	9	26	251
12	140,000	20,000	244	9	59	477
13	160,000	25,000	331	7	66	499

On the basis of these results, it would appear that multi-time-scale behavior exists. The weight is the slowest state, E is faster, and h and γ are the fastest. Finally, this assertion is also supported if one considers the maximum state rates achievable at each of these flight conditions. Maximum rates correspond to minimum time constants, which are shown in Table 3. Thus it is argued that the assumptions necessary to justify the energy-state approximation appear to be strongly supported in terms of the h and γ dynamics and weakly supported in terms of weight.

In a similar fashion, one may investigate the dynamic separation in the weight domain. This domain, of course, is relevant for minimum-fuel problems. Now define the characteristic weight constant

$$w_i = \left[\Delta x_i \Big/ \left(\frac{\mathrm{d}x_i}{\mathrm{d}W}\right)\right] = t_i \dot{W} = \left(\frac{t_i}{t_W}\right)\Delta W \tag{13}$$

in terms of the change of state per unit fuel burned. (Note that $\mathrm{d}W/\mathrm{d}W$ is unity.) By examining these parameters over the flight envelope, one obtains the same basic results. That is, altitude and flight-path angle have smaller characteristic weight constants compared with that of energy. The separation between the energy dynamics and the weight dynamics is present but is not as large as the separation between energy and the other states.

These results seem at first to contradict the results from Ref. 5, and some discussion is in order. The basic approach of the authors of Ref. 5 was first to rewrite Eqs. (4–7) in a form consistent with singular-perturbation analysis, or

$$\dot{E} = \frac{(\mathrm{Th}_{\mathrm{installed}} - D)V}{W} \tag{4}$$

$$\varepsilon \dot{h} = V \sin\gamma \tag{5'}$$

$$\varepsilon \dot{\gamma} = (g/WV)[L_{\mathrm{avail}} - W\cos\gamma] + [V/R]\cos\gamma \tag{6'}$$

$$\dot{W} = -\dot{W}_f \tag{7}$$

in which the singular parameter ε appears. Then a normalization of the right-hand sides was performed by nondimensionalizing all the variables using a selected set of constants S, where

$$S = (t_0, E_0, m_0, R_0, V_0, f_0, T_0, D_0, L_0)$$

The values for the elements in S were selected, for a particular vehicle and mission, such that each of the right-hand sides of Eqs. (4–7) was bounded by unity. Also, V_0 and Th_0/m_0 were selected such that both

$$V/V_0 \text{ is of order 1} \tag{14}$$

and

$$\frac{\mathrm{d}(E/E_0)}{\mathrm{d}t} \text{ is of order 1} \tag{15}$$

Finally, the result of this selection led, in Ref. 5, to an ε [in Eqs. (5′) and (6′)] equal to the following:

$$\varepsilon = \left(\frac{R^2_{\mathrm{sea\ level}}}{\mu}\right)\left(\frac{\mathrm{Th} - D}{m}\right)_{\max} \tag{16}$$

If the value this ε takes on is much smaller than unity, two-time scale behavior in Eqs. (4–7) is indicated for the vehicle and mission considered.

Note that the value of the preceding ε is essentially the maximum axial acceleration. And in the cited reference, the authors stated that if this axial acceleration was less than unity, two-time scale behavior could be assured. But, as noted previously in this paper, for this vehicle the axial acceleration is significantly greater than unity in some regions of the flight envelope. Therefore, under the algorithm of Ref. 5, time-scale separation cannot be assured. But the results in Tables 2 and 3 appear to support the assertion of time-scale (and weight-scale) separation.

The differences are, we believe, due to the following. First, the analysis we are suggesting does not rely on a single ε but on four time (or weight) constants, which might be considered to be four different ε. Furthermore, note that $\mathrm{d}(E/E_0)/\mathrm{d}t$ is proportional to the product of velocity and axial acceleration. But only $\mathrm{d}(E/E_0)/\mathrm{d}t$ must be bounded by unity in the Ref. 5 approach. This does not require that both V and axial acceleration be bounded [Eqs. (5′) and (6′)], only their product. And, in fact, numerical results (shown later) indicate that this product does tend to be small enough to lead to the time-scale behavior sought. Specifically, large axial accelerations occur at lower flight velocities.

Example Optimal Solutions

Both fuel-optimal and time-optimal trajectories have been estimated using the energy-state approximation. For comparative purposes, a fuel-optimal trajectory and a time-optimal trajectory were also obtained via nonlinear programming. The GESOP package[4] was utilized, and in both cases multiple shooting was employed as the solution algorithm.[10] For these numerical analyses, all four equations of motion, [Eqs. (4–7)], are enforced, and the continuous trajectory was approximated via discretization using 50 multiple-shooting nodes.

Optimal trajectories were sought for which the initial conditions are $h = 38{,}000$ ft and $V = 5800$ ft/s, and the initial weight is 300,000 lb. The terminal conditions correspond to low-Earth-orbital altitude and velocity, or $h = 200{,}000$ ft and $V = 25{,}000$ ft/s,

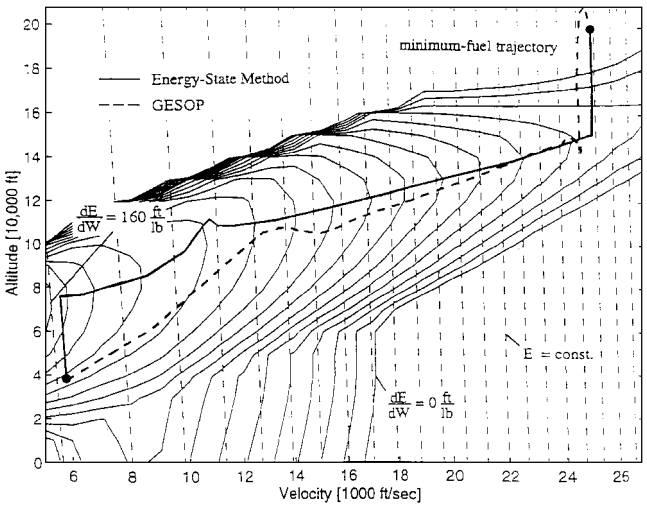

Fig. 6 Minimum-fuel trajectories.

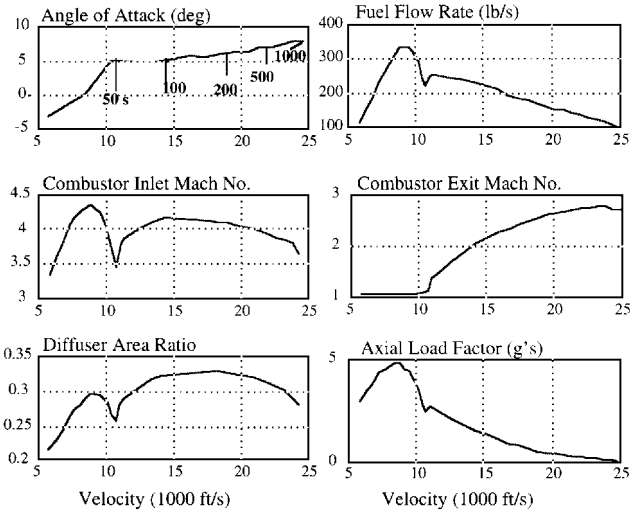

Fig. 7 Time histories along minimum-fuel trajectory.

and the terminal weight is to be maximized. The initial energy is $E_{\text{initial}} = 5.6 \times 10^5$ ft, and the terminal energy is $E_{\text{final}} = 9.9 \times 10^6$ ft.

The minimum-fuel solution obtained via the energy-state assumption is shown by the solid line in Fig. 6. These results are consistent with those of Ref. 11. Also shown are lines of constant energy (almost vertical dashed lines) and contours of constant $\mathrm{d}E/\mathrm{d}W_f$. The latter contours corresponding to smaller $\mathrm{d}E/\mathrm{d}W_f$ are closer to the $\mathrm{d}E/\mathrm{d}W_f = 0$ boundary of the flight envelope. The assumed constant weight used to solve for the angle of attack along the trajectory was 150,000 lb or half the initial weight. (If desired, one may iterate and change this weight after an initial solution has been obtained.) Note that the desired final orbital condition is outside the vehicle's flight envelope. Due to aerodynamic drag, this flight condition cannot be maintained indefinitely without using additional thrust. However, this flight condition can theoretically be reached, although not maintained, via a constant-energy zoom climb to the final flight condition. The fuel burned for this trajectory is estimated to be 160,000 lb, and the time required is about 1100 s. Finally, the time histories of key variables along the optimal trajectory are shown in Fig. 7. Of note are the large initial axial accelerations and fuel flow rates.

Also shown in Fig. 6 is the fuel-optimal trajectory generated via nonlinear programming, indicated by the heavy dashed line. For this solution, the flight time is 1142 s, and the total fuel burned is about 200,000 lb. Note that, at about 145,000 ft and at a velocity of 24,600 ft/s, a zoom climb to the final orbital condition with nearly constant energy height is indicated. This basic characteristic is consistent with that obtained by the energy-state method. The largest differences between the two trajectories occur during the early portion of the

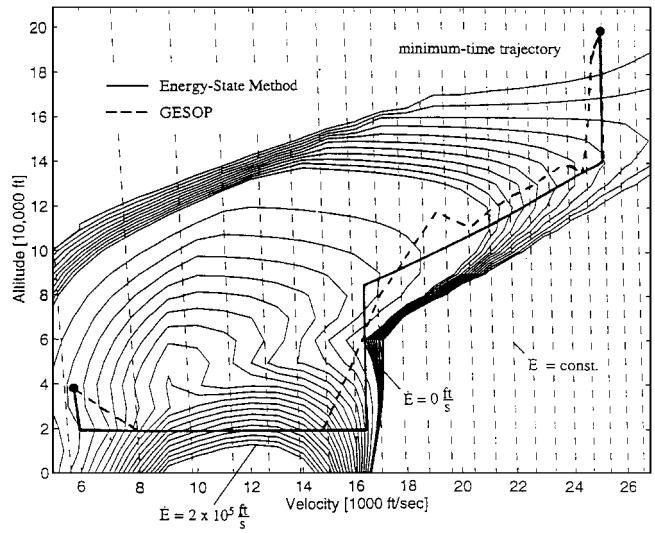

Fig. 8 Minimum-time trajectories.

trajectory. A zoom climb at the initial energy is not indicated in the nonlinear numerical solution.

Under the energy-state assumptions, recall that fuel required for a given energy change is minimized by maximizing $\mathrm{d}E/\mathrm{d}W_f$ at each energy level along the trajectory. This can lead to constant-energy trajectory segments, along which the vehicle is following a path of constant energy. In the results of Fig. 6, neither the initial flight condition nor the final flight condition corresponded to that yielding the maximum $\mathrm{d}E/\mathrm{d}W_f$ at the initial or final energy level, respectively. Therefore, under the energy-state solution, the optimal trajectory follows a constant-energy path until it achieves the maximum $\mathrm{d}E/\mathrm{d}W_f$ condition for that energy height. During such a constant-energy maneuver, the vehicle trades kinetic and potential energy with no net gain or loss in total energy. Such a maneuver requires zero time and fuel, because along a path of constant energy $\Delta E = 0$.

To complete the mission analysis, minimum-time trajectories were also generated. The energy-state solution is shown by the solid line in Fig. 8, where the initial and final conditions are the same as those used for the minimum-fuel trajectory. The fuel burned for this time-optimal mission is 264,000 lb, and the mission time required is 764 s. For this mission the vehicle was constrained to operate above 20,000-ft altitude.

Also shown in Fig. 8 is the corresponding nonlinear programming solution. This trajectory is also constrained to remain above an altitude of 20,000 ft. The fuel required in this case is 250,000 lb, and the mission time is 349 s. Except for the difference in time of flight, comparing the full-order numerical solution with the energy-state solution reveals strong qualitative agreement. The trajectories include a rapid initial descent to 20,000 ft, a steep ascent after accelerating to about 15,000 ft/s, and finally a zoom climb to the final orbital condition.

Conclusion

The optimization of the flight performance of a generic hypersonic vehicle is of interest, and the primary focus of the paper is assessing the validity of the energy-state approximation for this class of vehicle. Characteristic time constants and characteristic weight constants were introduced, and using this concept, an analysis of a selected, generic study vehicle indicated that multi-time-scale and multi-weight-scale behaviors exist over the entire scramjet-powered flight envelope of this vehicle. The argument for the existence of such behavior was, however, slightly weaker when considering the characteristic weight constants associated with vehicle weight and energy height. Energy-state solutions to the minimum-fuel and minimum-time single-stage-to-orbit trajectories were also compared with solutions obtained via nonlinear programming. These solutions showed rather good agreement. In particular, both solutions included a terminal zoom climb to the desired final flight condition. Based on these results, it would appear

that for this vehicle, as modeled, and for this mission phase the energy-state approximation is supported.

Acknowledgments

This research is supported in part by NASA Langley Research Center under Grant NAG 1-1540. The authors would also like to acknowledge Klaus Well, director of the Flight Mechanics Institute at the Technical University of Stuttgart, for his encouragement and for providing the GESOP software package.

References

[1]Schmidt, D. K., and Lovell, T. A., "Mission Performance and Design Sensitivities of Air-Breathing Hypersonic Vehicles," *Journal of Spacecraft and Rockets*, Vol. 34, No. 2, 1997, pp. 158–164; see also AIAA Paper 93-4009, Aug. 1993.

[2]Corban, J. E., Calise, A. J., and Flandro, G., "Rapid Near-Optimal Aerospace Plane Trajectory Generation and Guidance," *Journal of Guidance, Control, and Dynamics*, Vol. 14, No. 6, 1991, pp. 1181–1190.

[3]Kokotovic, P., Khalil, H. K., and O'Reilly, J., *Singular Perturbation Methods in Control: Analysis and Design*, Academic, New York, 1986.

[4]Jaensch, C., Schnepper, K., and Well, K., "Multi-Phase Trajectory Optimization Methods with Applications to Hypersonic Vehicles," Flight Mechanics Inst., Technical Univ. of Stuttgart, Stuttgart, Germany, Feb. 1993.

[5]Calise, A. J., Markopoulos, N., and Corban, J. E., "Nondimensional Forms for Singular Perturbation Analyses of Aircraft Energy Climbs," *Journal of Guidance, Control, and Dynamics*, Vol. 17, No. 3, 1994, pp. 584–590.

[6]Hermann, J. A., "SSTO Mission Analysis of a Generic Hypersonic Vehicle," Final Rept., Flight Dynamics and Control Lab., Univ. of Maryland, College Park, MD, Aug. 1995.

[7]Bryson, A. E., Desai, M. N., and Hoffman, W. C., "Energy-State Approximation in Performance Optimization of Supersonic Aircraft," *Journal of Aircraft*, Vol. 6, No. 6, 1969, p. 481.

[8]Bilimoria, K. D., and Schmidt, D. K., "An Integrated Development of the Equations of Motion for Elastic Hypersonic Flight Vehicles," *Journal of Guidance, Control, and Dynamics*, Vol. 18, No. 1, 1995, pp. 73–81.

[9]Ardema, M. D., and Rajan, N., "Separation of Time Scales in Aircraft Trajectory Optimization," *Journal of Guidance, Control, and Dynamics*, Vol. 8, No. 2, 1985, pp. 275–278.

[10]Bock, H. G., and Plitt, K. J., "A Multiple Shooting Algorithm for Direct Solution of Optimal Control Problems," Preprints of the International Federation of Automatic Control 9th World Congress (Budapest, Hungary), July 1984, pp. 243–247.

[11]Lovell, T. A., and Schmidt, D. K., "Mission Performance of Highly-Integrated Hypersonic Aircraft via Energy-State Analysis," AIAA Paper 95-3373, Aug. 1995.